MINERALOGICAL ANALYSIS OF VARIOUS LITHOLOGIES IN COARSE RYUGU SAMPLES USING TRANSMISSION ELECTRON MICROSCOPY. M. Matsumoto[1], J. Matsuno[2], A. Tsuchiyama[2,3], T. Nakamura[1], Y. Enokido[1], A. Miyake[4], S. Enju[5], K. Uesugi[6], A. Takeuchi[6], M. Yasutake[6], Y. Fujioka[1], A. Takigawa[7], S. Okumura[4], I. Mitsukawa[4], M. Sun[3], D. Nakashima[1], T. Morita[1], M. Kikuiri[1], K. Amano[1], E. Kagawa[1], H. Yurimoto[8], T. Noguchi[4], R. Okazaki[9], H. Yabuta[10], H. Naraoka[9], K. Sakamoto[11], S. Tachibana[7,11], S. Watanabe[12], Y. Tsuda[11]. [1]Tohoku University, Miyagi 980-8578, Japan, [2]Ritsumeikan University, [3]CAS, GIG, [4]Kyoto University, [5]Ehime University, [6]SPring-8, JASRI, [7]University of Tokyo, [8]Hokkaido University, [9]Kyushu University, [10]Hiroshima University, [11]ISAS, JAXA, [12]Nagoya University. (Email: m_matsumoto@tohoku.ac.jp).

Introduction: The Hayabusa2 spacecraft successfully collected asteroidal materials at two landing sites on the C-type asteroid 162173 Ryugu and brought them to the earth in December 2020. On-site investigations suggested that Ryugu is a rubble pile ubiquitously containing hydrous phyllosilicates and probably related to hydrous carbonaceous chondrites [1, 2]. Ongoing initial analyses of the returned samples have proven the observational insights and indicated that the samples are most similar to CI chondrites [3–8].

In this study, we performed transmission electron microscopy (TEM) on various lithologies discovered from millimeter-sized Ryugu stones by field emission scanning electron microscopy (FE-SEM) and synchrotron radiation-based X-ray nanotomography (X-nCT) at SPring-8. Here we report the results indicating different degrees and conditions of aqueous alteration among the Ryugu lithologies. We mainly focus on the results of TEM observations and details of the FE-SEM and the X-nCT results are given by other talks in this meeting [4, 9].

Samples and Methods: We analyzed Ryugu stones collected from both the fist and the second landing sites (Chamber A and C samples, respectively) [10]. FE-SEM and X-nCT analyses for many Ryugu stones suggest that the samples of the two landing sites are basically similar in mineralogy [4, 9].

We analyzed totally five TEM sections: one from Chamber A (A0063 grain), four from Chamber C (C0002, C0046, and C0103 grains). The TEM sections were prepared using Ga focused ion beam (Ga FIB) systems at Tohoku University (Versa 3D) and Kyoto University (Helios NanoLab G3 CX), and a Xe plasma FIB system at TOYO Corporation (AMBER X), and analyzed by TEMs at Tohoku University (JEM-2100F) and Kyoto University (JEM-2100F).

Results and Discussions: *Ryugu C0046-FO001:* A TEM section was prepared from a fragment of C0046 grain (C0046-FO001), which looks as a common Ryugu grain, shortly after the sample distribution from JAXA. The sample mainly consists of a phyllosilicate matrix with abundant embedded pyrrhotite and pentlandite (a few tens of nanometer to ~1 μm in size) and contains large Mn-Fe-bearing dolomites (~1–5 μm), apatite (~2 μm), and carbon-rich globules (~200–500 nm). No anhydrous silicate was observed in this sample. The phyllosilicates have Mg-rich compositions (Mg#: ~80–85) and vary in size. Coarse-grained phyllosilicates (<50 nm in width normal to (001) plane and >50 nm in length) having lattice spacing of ~0.70–0.73 nm and ~1.0–1.2 nm (indicate serpentine and saponite, respectively), bundles (~50–100 nm in thickness) of straightly elongated (~100–200 nm) serpentine (lattice spacing ~0.70–0.73 nm), and poorly crystallized fibrous silicates (<50 nm) are mixed in the matrix. Some dolomites are surrounded by well-developed serpentine (>50 nm in width normal to (001) plane and >200 nm in length). An aggregate (~2.5 μm) of poorly crystallized fibrous silicates and carbon-rich amorphous materials, and pyrrhotite attached with sphalerite (~100 nm) were also observed in this sample. These mineralogical characteristics, except for absence of magnetite, are similar to the major Ryugu lithology and CI chondrites [4, 5].

Ryugu C0002 plate-5 fragment-1: A TEM section was prepared from an olivine and pyroxene-bearing lithology (fragment 1) in the polished section C0002 plate 5 [4]. The sample mainly consists of a Mg-rich (Mg#: ~70–75) phyllosilicate matrix with abundant embedded pyrrhotite and pentlandite (a few tens of nanometer to ~1 μm in size) and contains some forsteritic olivines (~0.3–2 μm) and aggregates (~0.5–5 μm) of tochilinite-cronstedtite intergrowth (TCIs). The phyllosilicate matrix mainly consists of coarse-grained phyllosilicates (<50 nm in width normal to (001) plane and >50 nm in length) having lattice spacing of ~0.70–0.73 nm and ~1.0–1.2 nm (indicate serpentine and saponite, respectively), with minor poorly crystallized fibrous silicates (<50 nm). The edges of the olivines are commonly replaced by poorly crystallized fibrous silicates.

If we assume that all lithologies found in Ryugu samples were formed from a common precursor, the occurrence of remnant olivines in fragment 1 indicates a relatively low degree of aqueous alteration compared to C0046-FO001. In addition, the occurrence of TCIs, which are abundant in typical CM chondrites [11] but rarely occur in Ryugu samples, suggests that fragment

1 went thorough aqueous alteration at different condition from the major Ryugu lithology.

Ryugu C0002 plate-6 olivine-bearing lithology: An unique lithology, consisting of an olivine-rich matrix with embedded large (~30–60 μm) Mg-Na phosphates was discovered in the polished section C0002 plate 6 [4]. We made a TEM section at a boundary between the Mg-Na phosphate and the matrix. The Mg-Na phosphate show a shrunk texture with abundant nano-sized voids indicating degassing of volatiles. The matrix mainly consists of poorly crystallized fibrous silicates (<50 nm, Mg#: ~50–60) with embedded pyrrhotite and pentlandite (a few tens of nanometer to ~1 μm in size) and contains abundant forsteritic olivines (~0.2–1 μm) (Fig. 1). Some of the pyrrhotite occur as small whiskers (~100–200 nm in length). Most olivines have sharp outlines and seem to have escaped effects of aqueous alteration. One platy spinel (~500 nm) was also found in this sample.

The occurrence of olivines with sharp outlines and absence of coarse-grained phyllosilicates suggest that this lithology experienced the lowest degree of aqueous alteration among the samples examined in this study. It is noted that lithologies indicative of lower degrees of aqueous alteration compared to this lithology were identified in C0002 (fragments 4 and 5) [4].

Ryugu C0103-FC005: X-nCT analysis identified numerous veins running inside a fragment of C0103 grain (C0103-FC005) [9]. TEM observation revealed that the veins (a few microns in width and a few tens of microns in length) consisting of well-developed Mg-rich (Mg#: ~90) saponite (lattice spacing ~1.2–1.3 nm) cross cut a finer-grained phyllosilicate matrix. The mineralogy of the matrix is basically similar to C0046-FO001 other than presence of abundant magnetite with various morphologies (framboids, spherulites, and euhedral grains). One large (~10 μm) aggregate of Mg-rich serpentine (Mg#: ~70–80) with bastite texture, which is probably a pseudomorph of a large olivine or pyroxene aggregate, was also observed.

The saponite veins seem to have formed at the last stage of aqueous alteration, and this lithology would have experienced a higher degree of aqueous alteration compared to C0046-FO001.

Ryugu A0063-FC010: X-nCT analysis identified an unique aggregate of carbonate grains inside a fragment of A0063 grain (A0063-FC010) [9]. TEM observation revealed that the dolomite grains (~1 μm) embedded in a phyllosilicate matrix have euhedral shapes. The mineralogy of the matrix is most similar to C0103-FC005 except for absence of saponite veins. The carbonate grains were identified as Mn-Fe-bearing dolomite. Some of them are largely replaced by Mg-rich phyllosilicates (exact phase is not identified at this time) and exhibit rounded outlines. Some large rounded objects (~2–6 μm) consisting of similar Mg-rich phyllosilicates were also observed in the matrix. These would be pseudomorphs of large dolomite grains.

X-nCT analysis for many Ryugu samples indicates that dolomite formed at late stages of aqueous alteration [9]. The occurrence of largely replaced dolomite, which is absent in the other lithologies in this study, indicates a relatively high degree of aqueous alteration of this lithology.

Summary: The presence of multiple lithologies with different degrees of aqueous alteration in the Ryugu samples was inferred from this study. Among them, the less altered ones with anhydrous silicates may represent the precursor of the asteroidal materials in Ryugu. Further study for many other lithologies will reveal a series of aqueous alteration occurred in the asteroid Ryugu.

Acknowledgments: We appreciate TOYO Corporation for their assistance with the Xe plasma FIB sample preparation. The X-nCT analysis was conducted at SPring-8 BL47XU under the proposals 2021A0166 and 2021B0188 with supports by RIKEN.

References: [1] Watanabe S. et al. (2019) *Science, 364,* 268–272. [2] Kitazato K. et al. (2019) *Science, 364,* 272–275. [3] Yurimoto H. et al. (2022) *This meeting.* [4] Nakamura T. et al. (2022) *This meeting.* [5] Noguchi T. et al. (2022) *This meeting.* [6] Okazaki R. et al. (2022) *This meeting.* [7] Yabuta H. et al. (2022) *This meeting.* [8] Naraoka H. et al. (2022) *This meeting.* [9] Tsuchiyama A. et al. (2022) *This meeting.* [10] Tachibana S. et al. (2022) *This meeting.* [11] Tomeoka K. and Buseck P. R. (1983) *Nature, 306, 354–356.*

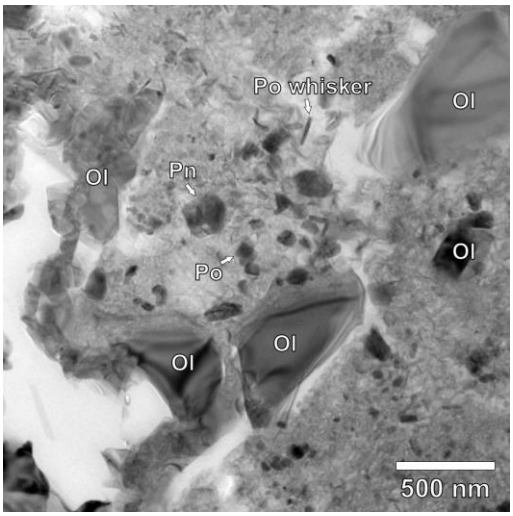

Fig. 1. TEM image of the unique olivine-bearing lithology in C0002 plate 6. A lot of olivine (Ol) grains occur in a poorly crystallized fibrous matrix. Pn = pentlandite, Po = pyrrhotite.